Automation in Construction 118 (2020) 103293

Contents lists available at ScienceDirect

Automation in Construction

journal homepage: www.elsevier.com/locate/autcon

Tunnel construction ventilation frequency-control based on radial basis function neural network

Rong Liu[a], Yi He[a,b], Yunfeng Zhao[a], Xiang Jiang[c,d,*], Song Ren[a,**]

[a] School of Resources and Safety Engineering, Chongqing University, Chongqing 400044, PR China
[b] School of Metallurgy and Materials Engineering, Chongqing University of Science and Technology, Chongqing 401331, PR China
[c] School of Civil Engineering, Chongqing University, Chongqing 400044, PR China
[d] University of Cambridge, Department of Earth Sciences, Downing Street, Cambridge CB2 3EQ, United Kingdom

ARTICLE INFO

Keywords:
Tunnel construction ventilation
RBF NN
Intelligent frequency control
Ventilation energy savings

ABSTRACT

Reasonable and effective ventilation plays an important role in the safety of tunnel construction. Fans are usually designed to be are capable of satisfying the maximum demand of a tunnel. During the tunnel construction, the actual usage of the tunnel could be considerably less than the designed fan capacity. This leads to high energy consumption and low efficiency. Therefore, a system that can analyze in real-time the tunnel environment and calculate the actual demand is required for tunnel construction. In this study, a tunnel ventilation intelligent frequency control (TVIC) system is designed based on the radial basis function neural network (RBF NN). As a type of feedforward neural network, RBF NN is used to obtain the relationship between the fan operating frequency and various pollutant concentrations, the tunnel length, and the temperature. TVIC is composed of a safety-monitoring system, control system, communication system, and variable-frequency drive (VFD) fan. It can self-adjust the frequency of the fan according to the construction environment inside the tunnel, and has been used in the Huayingshan tunnel in southwest China for a year and a half. In addition, it displays good reliability and a satisfactory capacity for tunnel environmental improvement and energy conservation. Compared with the current manual control method, ventilation system was observed to reduce electricity consumption by 42% after using TVIC.

1. Introduction

Following the implementation of China's central government policy of "*the development of the western region of China*," a large number of tunnels have been built in western China owing to the mountainous and hilly landscape. Tunnel ventilation is one of the main sources of energy consumption, both in the construction and operation stages. Many studies have focused on energy-saving control methods for tunnel ventilation systems during the operation period, such as the benefits of natural ventilation [1], fuzzy control model [2–4], and feed-forward control structure with an adaptive logic [5]. However, it is pretty rare about the smart strategy for ventilation in the construction stage.

During tunnel construction, hazardous gases (methane, carbon monoxide, and hydrogen sulfide) and dust are released into the tunnels [6–9]. Fresh air is delivered into the tunnel by fans to dilute the hazardous gases and dust. The type of fan is determined by the most difficult ventilation period, which indicates the maximum required air volume and the maximum air resistance. Therefore, the supply air volume and total pressure should be equal to or greater than the maximum required air volume and the maximum air resistance of the tunnel. The maximum number of workers, the explosive volume used in blasting, the minimum air velocity, and the total number of all internal combustion engines are normally considered in the calculation of the required air volume. Furthermore, if the tunnel crosses the gas-bearing strata, the supply air volume used to dilute the gas needs to be considered. The air resistance calculation is based on the maximum ventilation path. However, the duration of the maximum ventilation path is very short compared with the entire construction period, and there is not always a demand for the maximum required air volume. Therefore, the actual demand could vary and be much less than the designed capacity [10]. Moreover, fans will operate with a constant frequency when installed on a construction site. The above situations cause two

* Correspondence to: X. Jiang, School of Civil Engineering, Chongqing University, Chongqing 400044, PR China.
** Correspondence to: S. Ren, School of Resources and Safety Engineering, Chongqing University, Chongqing 400044, PR China.
E-mail addresses: cqu_liurong@cqu.edu.cn (R. Liu), yoyaheyi@cqu.edu.cn (Y. He), zhaoyf@cqu.edu.cn (Y. Zhao), jiangxiang@cqu.edu.cn (X. Jiang), rs_rwx@cqu.edu.cn (S. Ren).

https://doi.org/10.1016/j.autcon.2020.103293
Received 22 October 2018; Received in revised form 18 April 2020; Accepted 30 May 2020
Available online 06 June 2020

disadvantages, namely waste of the ventilation energy consumption and low effectiveness. To maintain a suitable underground environment and climate while reducing the cost of the ventilation system, the efficiency of ventilation systems needs to be improved [11–14].

Various speed control systems for fans have been developed in order to regulate air volume [15–19]. Most of these methods rely on variable-frequency drives (VFDs) to achieve rotation speed control. VFDs have been used in various applications, such as coolers and building management systems, owing to their effective energy conservation [20–23]. However, a VFD is only a speed adjustment device, and it cannot calculate the optimum running frequency. During the construction period, the tunnel environment is complex and variable. Therefore, a system that can analyze the tunnel environment and calculate the operating frequency of the fan is required [24,25].

With respect to the complex and variable construction environment, this paper presents a new tunnel ventilation intelligent frequency control system (TVIC) based radial basis function neural network (RBF NN), establishes the relationship between the tunnel fan operating frequency and tunnel environment. This system has been used in the Huayingshan Tunnel, southwest China, during the tunnel construction period.

2. Current status of tunnel ventilation technology in China

Based on the "*eight vertical and eight horizontal*" and "*71,118 network*" plans in China, the construction of railways and expressways has entered a new period of development. Fig. 1 shows the total mileage of railways and expressways every year. At the end of 2018, the total number of road tunnels was 17,738, covering a total distance of 17,236.1 km. Among them, the number of extra-long tunnels was 1058 with a total length of 4706.6 km. The number of long tunnels was 4315 with a cumulative length of 7421.8 km.

2.1. Difference in tunnel ventilation requirements during operation and construction periods

According to "*The Guidelines for Design of Ventilation of Highway Tunnel*" from the Ministry of Transport of the People's Republic of China [26], the maximum value of CO cannot exceed 100 cm^3/m^3 when the tunnel length exceeds 3000 m, and the tunnel visibility (indexed by transmittance in 100 m) needs to be $> 0.0065\ m^{-1}$ under normal traffic circumstances. During the tunnel operation period, the purpose of ventilation [27,28] is to change the chemical composition and climatic conditions of the atmosphere inside the tunnel to meet safe driving requirements. However, the purpose of ventilation during tunnel construction is to provide sufficient fresh air and suitable climatic conditions for the construction crew and mechanical equipment inside the tunnel, and to dilute the harmful gases and dust to safe levels [29–31]. Harmful substances include gases released from blasting, rock strata, and exhaust from construction machinery, such as carbon monoxide, nitrogen oxides, hydrogen sulfide, sulfurous anhydride, methane, and hydrogen sulfide [32]. While, the main harmful substances are vehicle exhaust and dust during the tunnel operation period [33,34]. The difference in tunnel ventilation between the operation and construction periods is illustrated in Fig. 2. Most of the vehicles in the tunnel are civilian cars, which have less pollution during the operation. However, tunnel construction in China involves the use of large diesel-powered construction equipment that emits significant amounts of pollution. Owing to the limitation of technology and conditions, fully electric engineering machinery is unable to replace diesel engine equipment [35–37]. The rock stratum is sealed during the tunnel operation period, but it is uncovered from the face during construction, and gases from the rock stratum can be directly released into the tunnel atmosphere. Besides, the tunnel is a semi-closed space during construction, which increases the difficulty of forming a ventilation circuit. During the operation period, the tunnel construction has been completed, and the length and air resistance are constant. In contrast, the tunnel length and the air resistance constantly increase during the construction period. Therefore, the fundamental differences in the ventilation between the operation and construction periods are the increased complexity of the ventilation, concentrated gases, and varying ventilation resistance. The above-mentioned differences imply that some recent research results that are applicable to the tunnel operation period cannot be directly applied to the construction period.

2.2. Ventilation status and existing problems associated with tunnel construction in China

Different automation and robotics technologies have been developed in the construction field [38], and tunnel construction technology in China has continuously improved, including in terms of construction speed and safety. However, the development of tunnel construction ventilation systems did not see similar progress. Ventilation systems are still operated in the "bystander" mode, i.e., fans are scarcely adjusted based on atmospheric changes inside the tunnel.

Press-in ventilation is a commonly used ventilation mode during tunnel construction in China [39]. In addition, the soft air ducts used in press-in ventilation are easily damaged. Damaged air ducts result in an insufficient air supply in the work zone as well as an eddy current that impedes the discharge of toxic and harmful gases and dust in the tunnel. Further, fans used on tunnel construction sites have only two working states: ON and OFF. These situations lead to low efficiency and high-power consumption. During tunnel construction, there is therefore the need for a smart ventilation system that can provide the required air volume according to the requirements of the tunnel environment and which can save power.

3. Algorithmic method

3.1. Smart ventilation system demand analysis

The air supply volume of the fan is determined by the real-time air volume required. The increased ventilation resistance should also be used to determine the pressure of the fan. Eq. (1) describes the relationship between environmental factors and the air volume of the fan and the operating pressure, respectively.

$$\begin{aligned} Q_{\text{fan}} &= f\left(C_{\text{Gas}_1}, C_{\text{Gas}_2}, C_{\text{Gas}_3} \cdots C_{\text{Gas}_n}, v_{\text{air}}, L, T\right) \\ H_{\text{fan}} &= f(R) \end{aligned} \tag{1}$$

where Q_{fan} is the air volume of the fan; H_{fan} is the operating pressure; C_{Gas} is the concentration of harmful gases; v_{air} is the air velocity in the tunnel; L is the tunnel real-time length; T is the temperature in the tunnel; and R is the resistance of the tunnel, which is proportional to the length of the tunnel.

According to the characteristics of the fan, the fan air volume is proportional to the rotation speeds, and the fan air pressure is proportional to the square of the rotation speeds. There is a positive correlation between the fan rotation speeds and the running frequency, and it can be expressed as follows:

$$\begin{aligned} &\frac{Q}{Q'} = \frac{n}{n'} \\ &\frac{H}{H'} = \left(\frac{n}{n'}\right)^2 \frac{\rho}{\rho'} \\ &n = 60\frac{\mathrm{f}_{\text{fan}}}{p} \Rightarrow \mathrm{f}_{\text{fan}} = \frac{np}{60} \end{aligned} \tag{2}$$

where Q and Q' are the air volumes of the fan at different rotation speeds, H and H' are the operating pressures at different rotation speeds, and n and n' are the different rotation speeds. ρ and ρ′ are the medium densities. f_{fan} is the fan operating frequency, and p is the number of pole pairs of the fan motor.

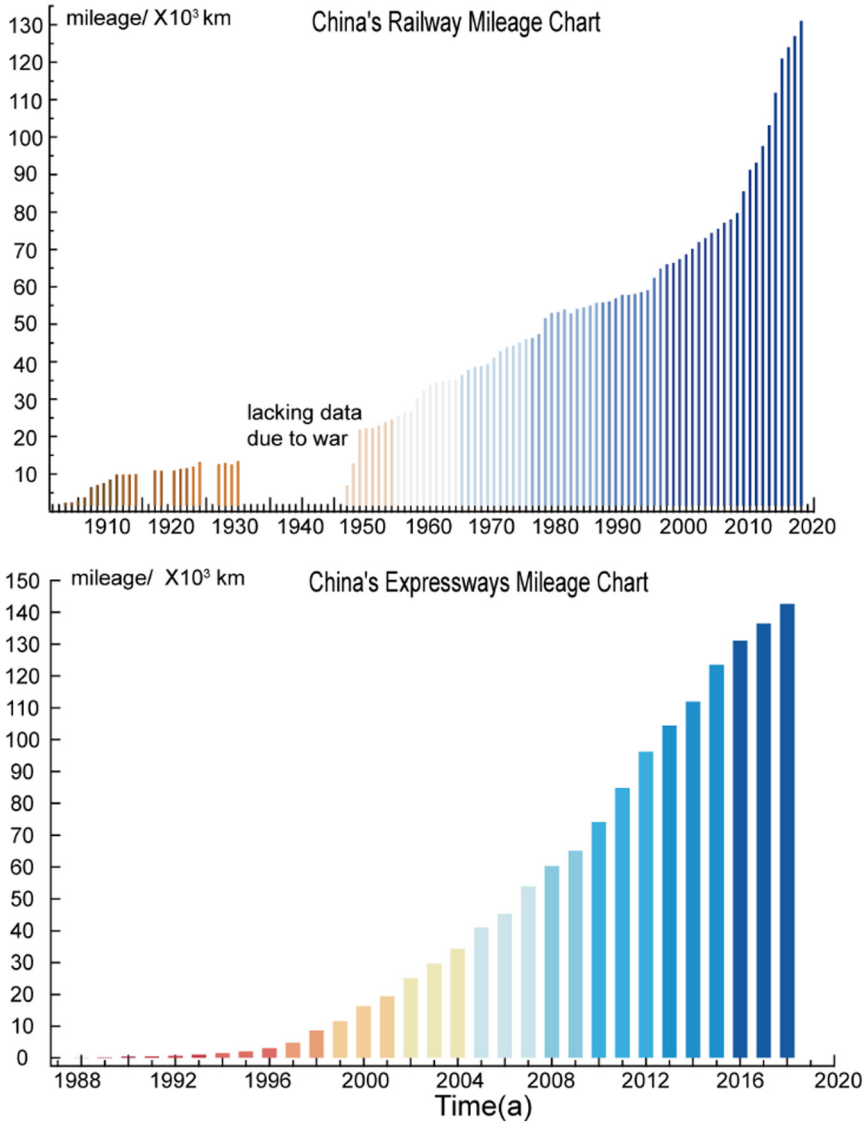

Fig. 1. Railway mileage and expressway mileage in China (data from the Statistical Bulletin of the Ministry of Transport, P.R. China).

From Eq. (2), for a fan:

$$Q_{\text{fan}} = f(\text{f}_{\text{fan}})$$
$$H_{\text{fan}} = f(\text{f}_{\text{fan}}) \quad (3)$$

By combining Eqs. (1) and (3), the following formula can be obtained.

$$\text{f}_{\text{fan}} = f(C_{\text{Gas}_1}, C_{\text{Gas}_2}, C_{\text{Gas}_3} \cdots C_{\text{Gas}_n}, v_{\text{air}}, L, T) \quad (4)$$

In this equation, the pressure is replaced by the tunnel temperature and length.

Such a ventilation system would not only meet the construction requirements, but would also eliminate unnecessary electricity use. Therefore, it is necessary to determine how to obtain the supply air volume and air pressure of the fan which matching with the concentration of various pollutants, tunnel length, and resistance. Many studies [40–43] have already explained the distribution and diffusion of pollutants under tunnel ventilation, but few studies have focused on the relationship between the pollutant concentration and air volume.

To determine the relationship between the tunnel fan operating frequency and the construction environment requirements, the Huayingshan Tunnel is selected as the research object. The Huayingshan Tunnel is a segment of an expressway from Chongqing to Guang'an. Fig. 3 shows the geographical location of the Huayingshan Tunnel; the entrance is located in Beibei District, Chongqing. The exit is in Hechuan District, Chongqing. The lengths of the left and right tunnels are 5018 m and 5000 m, respectively. Table 1 shows the performance parameters of the fan used in the Huayingshan Tunnel. The air volume of the fan ranges from 41.8 m^3/s to 85.0 m^3/s, and the pressure ranges from 697 Pa to 4571 Pa. The tunnel was classified as a gas tunnel based on geological exploration. The strata of the Huayingshan Tunnel contain methane and hydrogen sulfide. Therefore, the levels of methane, hydrogen sulfide, carbon monoxide, temperature, and air velocity were monitored in the tunnel.

3.2. RBF neural network background

Owing to its simple topological structure and good ability to approximate any nonlinear function with arbitrary precision [44-46], the RBF NN was used to determine the relationship between the fan operating frequency and various pollutant concentrations, the tunnel length, and the resistance. RBF NN is a type of feedforward neural network that learns using a supervised training technique and comprises three different layers: an input layer, a hidden layer, and an output layer. RBF is used as the “basis” of the hidden layer neuron to form the hidden layer space. The input vector can be directly mapped to the hidden layer

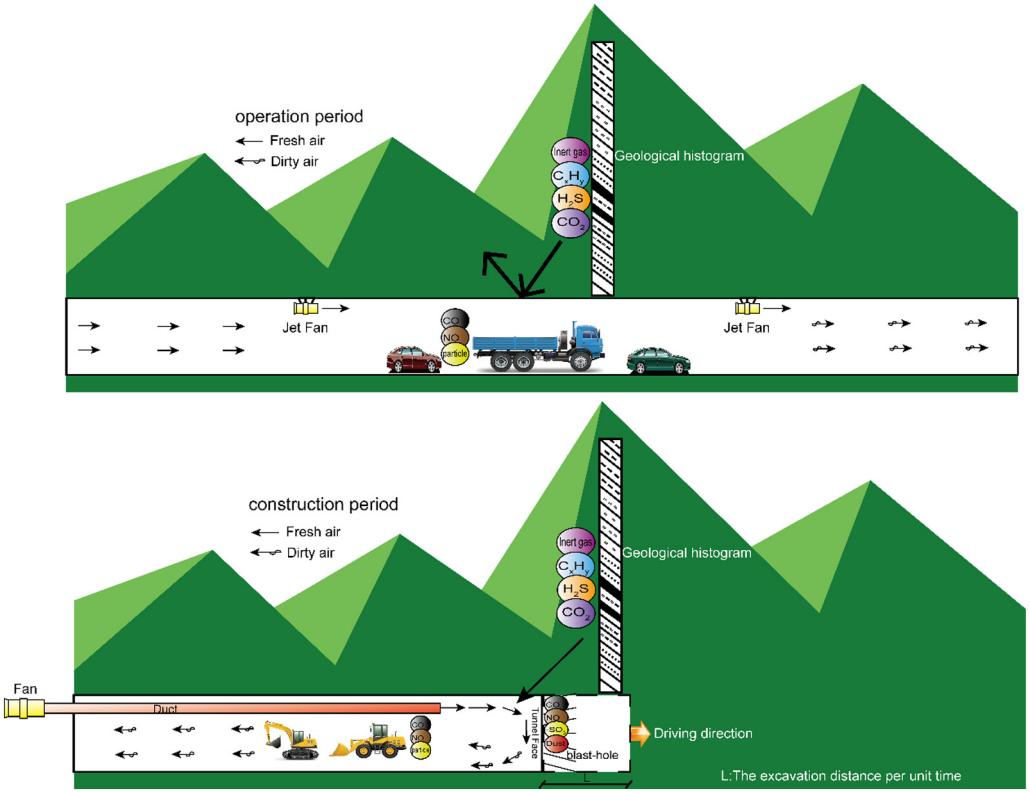

Fig. 2. Differences in tunnel ventilation between the operation and construction periods.
(The tunnel during the operation period has been completed, but the tunnel during the construction period is still being constructed.)

space without passing the "weight" connection. Once the center point of the RBF is confirmed, the mapping relation is also determined. The mapping from the hidden layer space to the output space is linear, that is, the network is a linear weighted sum of the output of the hidden layer neurons. Here, "weight" is a network tunable parameter. The network from the input layer to output layer, the mapping relationship is non-linear, and the network output is linear for tunable parameters. The "weight" of the network can be directly solved by the linear equation; thus, the learning speed can be accelerated, and the local minimum problem can be avoided [47,48].

RBF NN has been shown to be suitable for solving problems involving multiple inputs and a single output [48]. For example, RBF NN was applied to evaluate the interference effects (expressed by the interference factor) among adjacent buildings under wind action, using 106 sets of data. The input layer contains the relationship between the buildings' relative locations, building height ratio, and upstream terrain condition. The output is expressed in terms of the interference factor [44]. Compared with other learning algorithms, RBF NN will obtain better results in solving such problems because its training procedures are very fast, and it does not encounter the local minima problems [49,50].

3.3. Training data set acquisition

Training a neural network requires a training data set (TDS). According to a study on TDSs, the neural network involves an implicit relationship between the input and output. In this study, the pollutant concentration, length of the tunnel, and temperature are considered as the input layer, and the fan operating frequency is considered as the output layer. However, there is no data set to describe the relationship between these layers. The maximum allowable concentration or range of pollutants can be obtained only from the *Technical Regulations for Railway Gas Tunnels* and *Safety Regulations in Coal Mine* [51,52]. Table 2 lists the allowable values of environmental parameters and air velocity that are monitored in the Huayingshan Tunnel.

In order to obtain TDS, fan response rules based on the tunnel environment were formulated, as shown in Table 3. The tunnel environment is divided into five stages based on the gas (CH_4, CO, and H_2S) concentrations. In Stage 1, the concentrations of the three gases are between 0 and the intrinsic error of instruments. For field applications, the pollutant concentration is regarded as close to zero in Stage 1; the fan will operate at the basic frequency, which refers to the minimum frequency required to maintain a safe atmospheric tunnel environment. The basic frequency is determined by the amount of air volume required to meet the minimum air velocity, the tunnel length, and the number of workers together in the tunnel. In Stage 5, at least one kind of gas has exceeded the allowable values specified in the specification. At this stage, the fan should run at the rated frequency, which refers to the maximum operating frequency of the fan, i.e., 50 Hz.

The concentration between the intrinsic error and the allowable value is divided into three cases (Stages 2–4). In these three cases, if the fan is operated at the rated frequency, it will inevitably result in a waste of electric energy. If it is operated according to the basic frequency, it may cause an increase in the gas concentration. Therefore, the fan should operate at an appropriate frequency value to dilute the gas for a specified period of time to the appropriate concentration range. To determine the appropriate operating frequency of the fan, the dilution time is used as a standard. Table 3 shows that when the concentrations of the three gases are in Stage 2, the appropriate fan operating frequency should be such that the gas concentration can be reduced to Stage 1 within 30 min. Similarly, when the concentration of the three gases is in Stage 3(4), the appropriate fan operating frequency should be such that the gas concentration is reduced to Stage 2(3) within 20(15) min. It is important to note that when the concentrations of the three gases are at different stages, the response action of the fan is determined by the maximum stage of the gas. Besides, when the temperature inside the tunnel exceeds 28 °C, the operating frequency of the fan increases until the temperature drops below 28 °C. From the

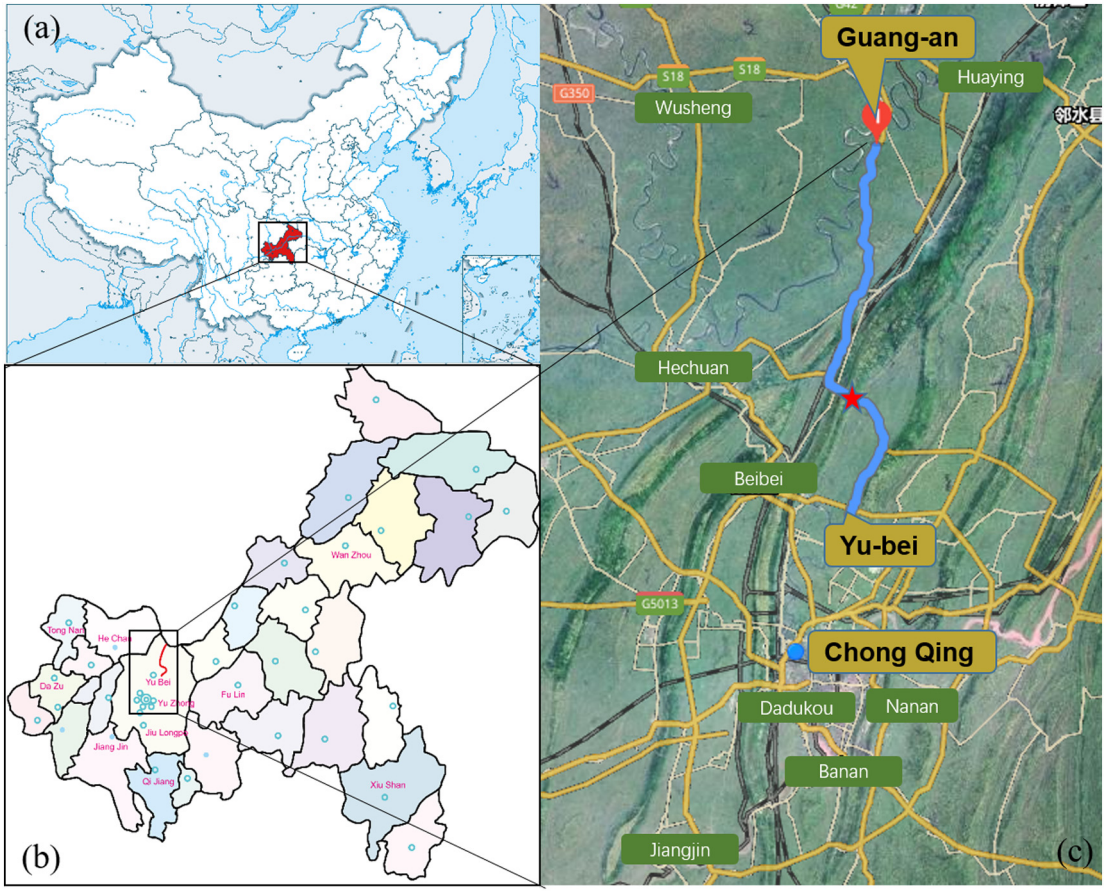

Fig. 3. Location of the Huayingshan Tunnel. (a) map of China, (b) map of Chongqing, (c) map of the expressway from Chongqing to Guang'an, where the Huayingshan Tunnel is shown by the red star. (For interpretation of the references to colour in this figure legend, the reader is referred to the web version of this article.)

Table 1
Fan parameters.

Impeller diameter (mm)	Rotation speed (r/s)	Air volume (m^3/s)	Pressure (Pa)	Efficient blast volume (m^3/s)	Motor (kW)	Duct (mm)
1700.0	1.3	41.8–85.0	697.0–4571.0	66.4	160.0 × 2	1800.0

Table 2
Allowable values of tunnel environmental parameters and air velocity.

Name	Allowable value
CH_4	0.5%
H_2S	6.6 ppm
CO	24 ppm
Air velocity	0.25–6 m/s
Temperature	28 °C

aforementioned rules, the operating frequency of the fan corresponding to the environmental parameters in the tunnel is obtained, and these constitute the TDS.

The TDS is obtained at the Huayingshan Tunnel using the aforementioned process, which is known as the TDS acquisition rules. Environmental parameters are obtained using a safety monitoring system and hand-held detector. The measuring range and accuracy of sensors are shown in Table 4. The fan frequency can be adjusted to meet the corresponding gas concentration through the manual control mode of TVIC, and it can be recorded. Depending on TDS acquisition rules, it takes about 15 to 30 min to get a set of data. According to the

Table 3
Data acquisition standard table.

Stage	CH_4 concentration (%)	H_2S concentration (ppm)	CO concentration (ppm)	Corresponding fan response action
1	0.0–0.1	0.0–0.5	0.0–1.0	Basic frequency
2	0.1–0.3	0.5–3.0	1.0–10.0	Reduced to Stage 1 within 30 min
3	0.3–0.4	3.0–5.0	10.0–18.0	Reduced to Stage 2 within 20 min
4	0.4–0.5	5.0–6.6	18.0–24.0	Reduced to Stage 3 within 15 min
5	> 0.5	> 6.6	> 24.0	Rated frequency

Table 4
Sensor performance parameters.

Gas name	Product model	Measuring range	Intrinsic error	Manufacturer
CH_4	KG9701B	0.00%–4.00%	± 0.10%	China Coal Technology Engineering Group Chongqing Research Institute
H_2S	GLH200	0 ppm–200 ppm	± 0.5 ppm	
CO	GTH1000	0 ppm–1000 ppm	± 1 ppm	
Air velocity	GFY15	0 m/s–15 m/s	± 0.1 m/s	Tiandi (Changzhou) Automation Co., Ltd
Temperature	KG3007A	−5 ℃ − +45 ℃	± 0.1 ℃	
Notice	Sensors will drift after being used for a period, so they need to be calibrated regularly. When a sensor is calibrated, the sensitive components need to be surrounded by the "Standard gas" [47]. After the value of the sensor is stable, the display value is adjusted to the concentration value of the "Standard gas." In China, the "National Safety Production Mining Equipment Inspection and Inspection Center" can provide the "Standard gas," which could be seen as the "true value," and which is used in this study.			

construction plan, two-shift cycling in one day operation has been adopted. One cycle contains four construction processes (Drilling-Blasting Method: drilling, blasting, mucking, and lining), and we choose blasting process to collect data since this stage is usually the peak level of concentration. This way can make the intensity of construction is relative stable among the data collections. During the process of TDS acquisition, the tunnel length increased from 1149 m to 1327 m (two months), and went through high gas and low gas segment. Finally, 76 sets of data were selected; these cover different gas concentrations and tunnel lengths.

3.4. Experimental procedure

The network structure that depicts the construction environment requirements is shown in Fig. 4. The calculating program was coded in MATLAB. The RBF NN has six inputs, namely C_{CH_4}, C_{H_2S}, C_{CO}, v_{air}, L, and T, and its matrix form is represented by

$$\boldsymbol{P} = \begin{bmatrix} C_1(\mathrm{CH_4}) & C_1(\mathrm{H_2S}) & C_1(\mathrm{CO}) & v_1(\mathrm{air}) & L_1 & T_1 \\ C_2(\mathrm{CH_4}) & C_2(\mathrm{H_2S}) & C_2(\mathrm{CO}) & v_2(\mathrm{air}) & L_2 & T_2 \\ \vdots & \vdots & \vdots & \vdots & \vdots & \vdots \\ C_M(\mathrm{CH_4}) & C_M(\mathrm{H_2S}) & C_M(\mathrm{CO}) & v_M(\mathrm{air}) & L_M & T_M \end{bmatrix} \tag{5}$$

where M represents the number of training set samples, and C_{CH_4}, C_{H_2S}, and C_{CO} represent the concentrations of CH_4, H_2S, and CO, respectively.

The output matrix form of training set samples can be expressed as

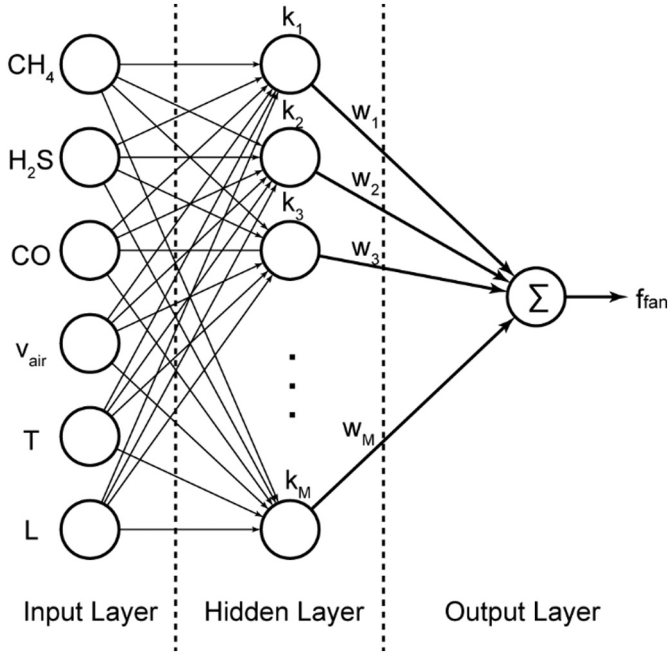

Fig. 4. Schematic representation of RBF-NN.

$$\boldsymbol{T} = [\mathrm{f}_1\ \mathrm{f}_2\ \cdots\ \mathrm{f}_M]^T \tag{6}$$

The multivariate Gaussian function is used as the activated function in the hidden layer of RBF NN, and its formulation is as follows [53].

$$k_j = \exp\left\{\frac{-\|\boldsymbol{p}_j - C\|^2}{2\sigma^2}\right\},\ j = 1, 2, \ldots M \tag{7}$$

where $\boldsymbol{p}_j = [C_j(\mathrm{CH_4})\ C_j(\mathrm{H_2S})\ C_j(\mathrm{CO})\ v_j(\mathrm{air})\ L_j\ T_j]$ is the j-th training sample vector; C represents the RBF centers; $\|\boldsymbol{p}_j - C\|$ is the norm value, which is measured using the inputs and the node center at each neuron; and σ is the node variance of the j-th neuron.

The RBF NN output can be written as [53].

$$\omega_{RBF} = \sum_{j=1}^{M} w_j k_j \tag{8}$$

where ω_{RBF} is the output value, and w_j and k_j are the weight and output of the j-th neuron, respectively.

In RBF NNs, the training algorithm is used to determine the optimal cost function minimizes the specified error between the output of the NN and the desired output. The gradient descent (GD) method is used to train the NN owing to the advantage of faster computation [54–56]. The number of neurons in the middle layer needs to be increased until the output error of the network equals the pre-set value. For the GD training process, the error instantaneous cost function is defined as [56].

$$J = \frac{1}{2}(\omega_{T(j)} - \omega_{RBF(j)})^2 \tag{9}$$

where ω_T is the true value of the j-th sample.

Then, according to the GD method, the weights are derived as follows:

$$w_{j+1} = w_j - d_j \cdot \eta_j \tag{10}$$

$$d_j = \omega_{T(j)} - \omega_{RBF(j)} \tag{11}$$

where $j = 1, 2, \ldots M$, and η is the learning rate.

To obtain the optimal solution of the GD method faster, an original value is mapped to the value of the interval [0, 1] by maximum-minimum normalization before training, and its formulation is as follows.

$$x_{normalization} = \frac{x - Min}{Max - Min} \tag{12}$$

where x represents the collected data, and Min and Max are the minimum and maximum value of this type of data, respectively.

3.5. Results of the algorithmic method

During training, 68 sets of data were randomly selected as the training set, and the remaining eight sets of data were utilized as the test set. The determination coefficient R^2 was utilized to evaluate the performance of the RBF-NN model. The formulation of this parameter is represented below [47]:

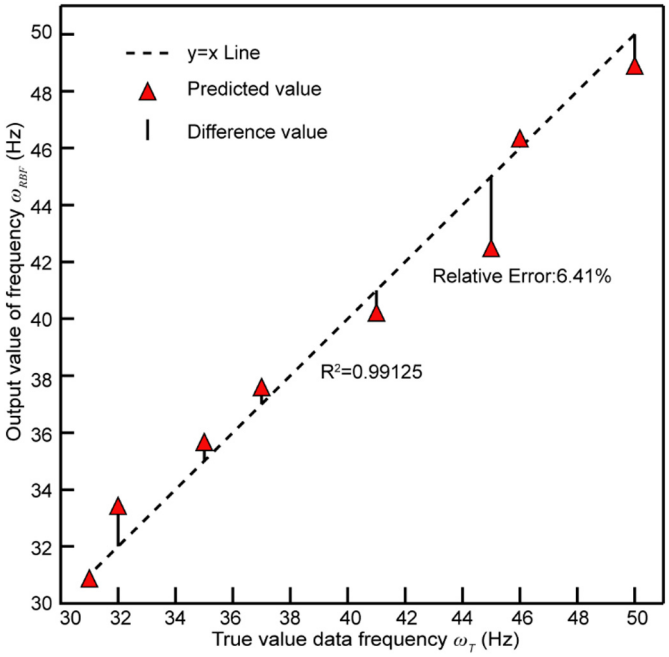

Fig. 5. Plot of output value of frequency against true data.

$$R^2 = \frac{\left[l \cdot \sum_{i=1}^{l} \omega_{RBF(j)} \omega_{T(j)} - \sum_{i=1}^{l} \omega_{RBF(j)} \cdot \sum_{i=1}^{l} \omega_{T(j)} \right]^2}{\left[l \cdot \sum_{i=1}^{l} \omega_{T(j)}^2 - \left(\sum_{i=1}^{l} \omega_{T(j)} \right)^2 \right] \cdot \left[l \cdot \sum_{i=1}^{l} \omega_{RBF(j)}^2 - \left(\sum_{i=1}^{l} \omega_{RBF(j)} \right)^2 \right]} \quad (13)$$

where l is the number of samples. The determination coefficient R^2 is between 0 and 1. The closer the determination coefficient is to 1, the better is the performance of the model.

The output value of the frequency was plotted against the true value data, as shown in Fig. 5. This figure shows that the true value data and output data are uniformly distributed around the unit slope line (y = x line). This means that there is a good agreement between model outcomes and target viscosity data. The determination coefficient R^2 of model predictions exceeds 0.99. The figure also shows that the maximum relative error is 6.41%, which means that the model predicts the target data accurately.

4. Building of the intelligent frequency control ventilation system

The above section introduced the algorithmic method applied to determine the fan operating frequency. The algorithmic method requires matched hardware and software to achieve full functionality. In this section, the software and hardware components are described.

4.1. System control method

TVIC comprises four subsystems: the safety monitoring system, the control system, the communication system, and a VFD fan. Fig. 6 shows the structure chart of the TVIC. The safety monitoring system is responsible for the real-time monitoring of the environment parameters in the tunnel. The control system uses the RBF NN training results to calculate and analyze the required operating frequency. The communication system converts the signals of the control system into signals that the VFD can recognize. The VFD and fan in the Huayingshan Tunnel are shown in Fig. 7. The communication devices and VFD fan used in this study are mature products, which are popular on the Chinese market.

The system working process is shown in Fig. 8. This process begins to operate after the self-test. The self-test aims to detect whether the entire system is complete and intact, and this test must be performed before the system operation begins. After the self-test, the basic frequency is calculated. Then, the control system reads the safety monitoring system data, calculates the result, and sends them to the VFD fan. The calculation and analysis method are based on the trained RBF NN. In addition, considering the fan service life, a frequent or sudden variation in the operating frequency will increase fan bearing abrasion. Therefore, a function is added to the programming method to address this issue. When the difference between the calculated frequency and the actual operating frequency of the fan is < 3 Hz, the calculated frequency will not be sent to the fan; when this value exceeds 3 Hz, the calculated frequency will be sent to the fan. According to previous experiments, the changes of air volume and air pressure are small when the fluctuation in the fan frequency is lower than 3 Hz. To avoid repeated frequency changes, 3 Hz is chosen as the threshold.

4.2. System hardware components

In the TVIC, safety monitoring systems are relatively well-researched systems that have been already applied in tunnel construction. Fig. 9 illustrates a structure chart of the safety monitoring system. The central computer is placed in the monitoring room outside the tunnel and is connected to the gas sensor via signal converters and substations. Signal converters are used to convert electrical signals to digital signals. The substation is used to power the sensor and transmit signals. Substations are connected to sensors and placed at different locations, including the tunnel face, the secondary lining construction area, and the return air course. In the Huayingshan tunnel, there were three CH_4 sensors, three H_2S sensors, two CO sensors, one air velocity sensor, and one temperature sensor at the tunnel face. At the second-layer liner construction area, there were three CH_4 sensors, two H_2S sensors, two CO sensors, one air velocity sensor, and one temperature sensor. At the return air course, only one CH_4 sensor and one air velocity sensor were installed.

The control system is the core component of the TVIC, and it performs data interpretation, calculations, and analysis. The controller is composed of an amplifier circuit, an analogue switch, a programmable logic controller (PLC) system, a power circuit, and a signal output circuit. These components are common and mature on the market. The controller is mainly involved in the following tasks: (1) Calculation and analysis functions – The control system reads the data from the safety monitoring system and uses the trained RBF NN to calculate the running frequency of the fan. (2) Turning the fan on and off – The system can control the ON/OFF switch of the fan. Moreover, the VFD can replace the soft starter. (3) Fan operation monitoring and fault alarms – The system monitors the fan operation, such as the voltage, the current and power parameters. Therefore, electrical accidents can be quickly identified. (4) Switch TVIC control and manual control – The system must have both a TVIC control mode and manual control mode. The two modes are set because of the legal requirements in China, and in consideration of special circumstances and special requirements. For example, the manual control mode is needed during the gas drainage process.

4.3. Software function and composition

The software that was applied in TVIC consists of two components: a control software and a human-computer interaction software. The control software is embedded in the controller and is involved in data input/output operations, calculations, and data analyses. These processes were presented in a previous Section 4.2.

The human-computer interaction software performs the following functions: displaying various parameters, ensuring the conversion between TVIC control and manual control, receiving and sending manual control parameters, and saving the parameters. The software interface is divided into four parts, i.e., a system login interface, a safety

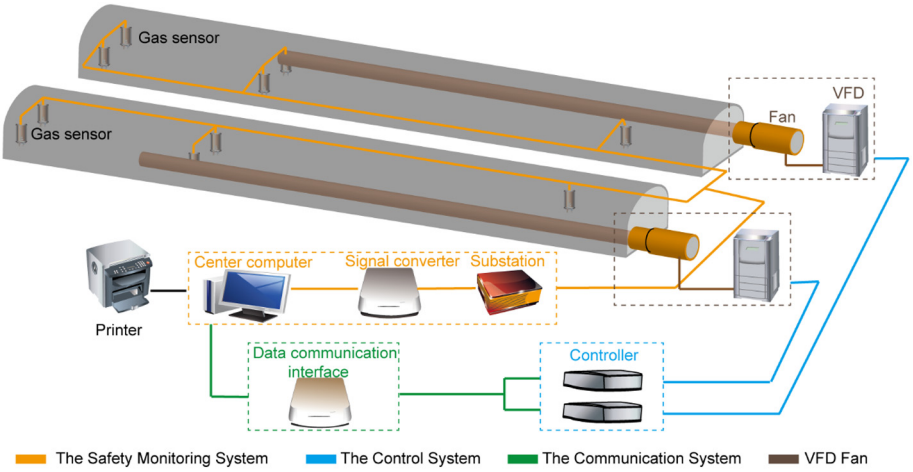

Fig. 6. TVIC structure diagram.

monitoring system display interface, a fan operating parameter display and manual control interface, and a help interface. Users can only start the software using a correct login password. The operation of the fan has a considerable influence on the atmospheric environment in the tunnel, and should guarantee its safety. This function mainly prevents unauthorized personnel from operating and controlling the fan. The second part of the software is the display interface of the safety monitoring system. The data from all of the sensors in the tunnel are shown on this interface. If the sensor values exceed specified allowable values, a beeping and flashing alarm will be triggered. The third part is the fan operating parameter display and manual control interface. In this part, the fan operating parameters are shown on the interface. The changeover switch button of TVIC control mode and manual control is also on the interface. After a manual modification of the frequency in the interface, the new frequency will be sent to the VFD fan after entering the correct password. All data will be stored on the central computer as a file, and anyone with permission can access this file via the Internet. The fourth part is the help interface.

4.4. Field test and application

4.4.1. Short-term on-site ventilation test

The TVIC was commissioned and installed in the Huayingshan Tunnel on June 15, 2015. Short-term (one week) tests of the stability and energy savings of the TVIC began at the entrance working section of the tunnel at 17:30 on June 29th, and ended at 17:30 on July 6th. At the beginning of the test, the length from the portal to the face on the left and right tunnels was 1381 m and 1403 m, respectively. The same construction method was used for the left and right tunnels throughout the test, so the environments were similar, ensuring the feasibility of the comparison experiment. The left and right tunnel fan control modes are shown in Table 5. The left tunnel had a manual control mode, which is currently a commonly used conventional ventilation method, while the right tunnel had the TVIC control mode. Before starting and after the end of the experiment, the electricity meter (Unit: kWh, Special electric meter for the fan) of the left tunnel fan showed 004692.1 and 004840.8 respectively, with a difference of 148.7. The electricity meter (Unit: kWh, Special electric meter for the fan) of the right tunnel fan showed 009923.0 and 010010.0 respectively, with a difference of 87. The electricity meters were linked to a mutual inductor during construction; hence, the actual ventilation energy consumption is the meter value multiplied by the rate 100. The actual electricity consumption on the left and right tunnels of the twin-tunnel is shown in Table 5. The table shows that the energy consumption for the right tunnel is only 58.5% of that for the left tunnel. It is easy to determine whether the TVIC mode provides a better energy-saving effect than the manual control mode.

4.4.2. Reliability, sensitivity and energy savings of TVIC

The reliability and sensitivity of the TVIC are evaluated based on actual operational data. After the short-term test was completed, the TVIC control modes were both used in left and right tunnels. Fig. 10 shows the concentrations of various toxic and harmful gases and the air velocity in two ventilation patterns. It should be noted that once the concentration of certain gases rises, the air velocity immediately increases. This good correlation shows the good reliability of this smart system. The increased air velocity indicates that the air volume of the fan increases and provides more fresh air to dilute and discharge the toxic and harmful gases. The maximum concentrations of CO reached 660 ppm and 820 ppm, while those of the other two gases were low.

Fig. 7. Photo of the fan and VFD.

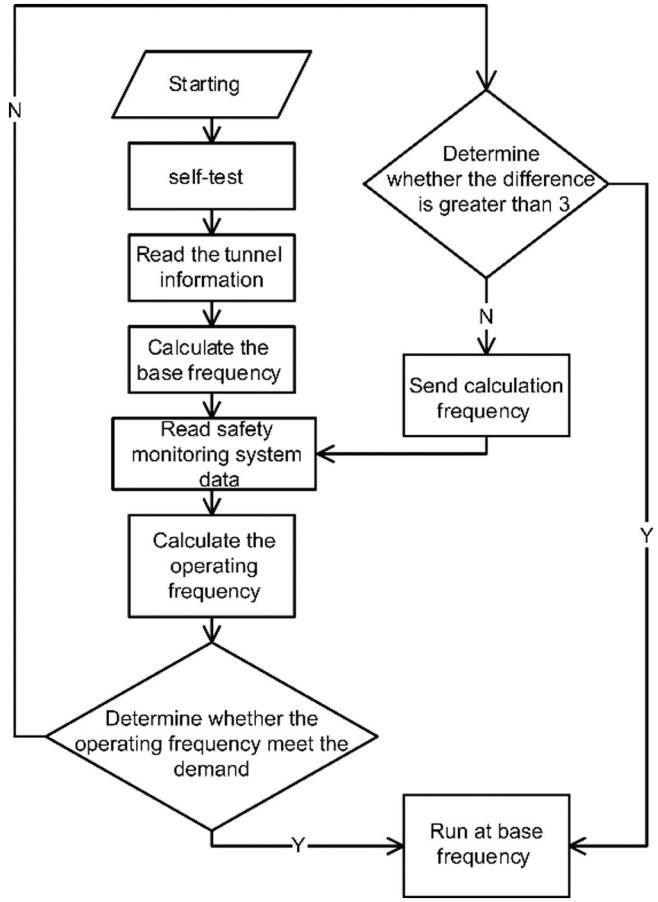

Fig. 8. System work process.

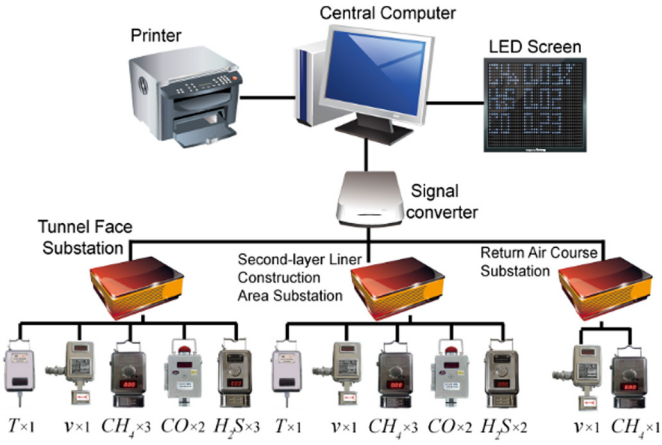

Fig. 9. Structure diagram the safety monitoring system.

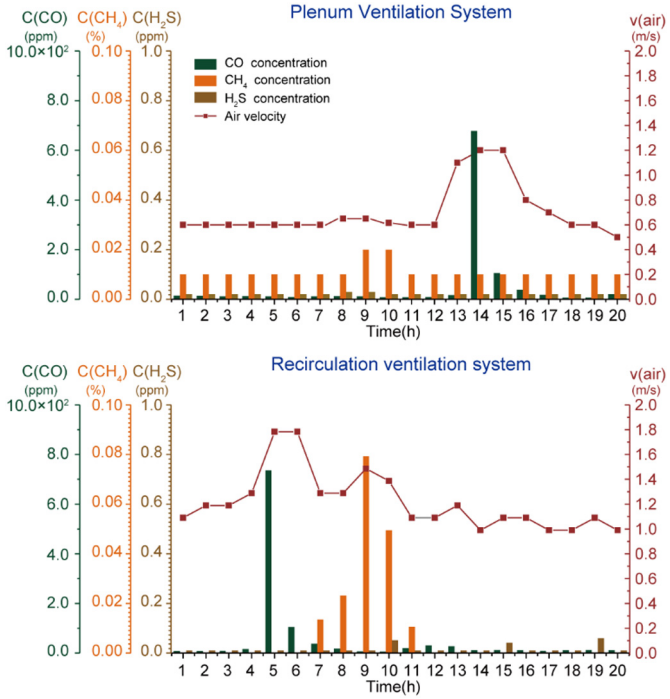

Fig. 10. Diagram of the pollutant concentrations and air velocity.

Two ventilation patterns (press-in ventilation and gallery-type ventilation system) were used in the early and late stages of the Huayingshan Tunnel, and both ventilation patterns employed the TVIC. It is obvious that TVIC improves the sensitivity of the fan.

The degree of the ventilation energy consumption of the Huayingshan Tunnel from January 2015 to August 2016 is shown in Fig. 11. The hollow column represents the monthly ventilation energy consumption before the use of TVIC. The solid column represents the monthly ventilation energy consumption after the use of TVIC. The ventilation energy consumption in June 2015 was 75,610.47 kWh in the right tunnel, while it was 43,356.98 kWh in July after using the TVIC. The electricity consumption for the ventilation process was reduced by nearly 42%. As the construction time increased, the tunnel depth and air resistance increased. Thus, the electricity consumption should increase according to a certain gradient, which can be seen from the nearly fixed rate of growth of the electricity consumption per month before using TVIC or after using TVIC. Compared with the case before using TVIC, the rate of growth of the electricity consumption per month also slowed significantly, which can be seen from the change in the slope (3142.3 kWh per month reduced to 1291.9 kWh per month in the left tunnel). The energy consumption savings were estimated to be about 1,426,000 kWh ($177,663.00, USD) when the TVIC was used during the overall construction period.

4.4.3. Cost-benefit analysis

Compared with the existing method, TVIC adds safety monitoring systems, VFD, and control systems. The investment increases owing to

Table 5
Tunnel fan mode in short-term on-site test and its energy consumption record.

	Left tunnel	Right tunnel
Control mode	Manual control: The fan manager adjusts the fan operating frequency according to the safety monitoring system data.	TVIC control: The control system performs calculations and analysis, and controls the operating frequency.
Start (kW·h)	004692.1	009923.0
End (kW·h)	004840.8	010010.0
Rate	100	100
Actual energy consumption (kW·h)	14,870.0	8700.0

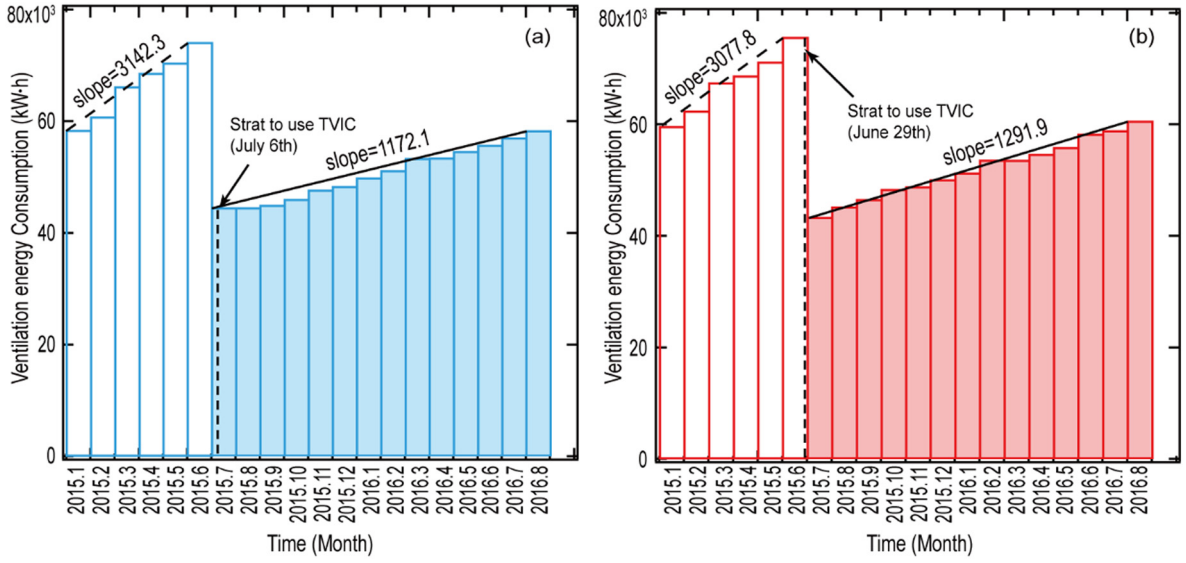

Fig. 11. Power consumption before and after TVIC installation in the Huayingshan Tunnel.
(a): Left tunnel, (b): Right tunnel.
(The hollow column represents the monthly ventilation energy consumption before the use of TVIC. The solid column represents the monthly ventilation energy consumption after the use of TVIC.)

Table 6
Installation cost and material cost of systems (Unit is in USD).

Items	Conventional ventilation method (manual control mode)			TVIC		
Fans	Unit price	Number	Total price	Unit price	Number	Total price
	20,706.00	1	20,706.00	20,706.00	1	20,706.00
VFD	Unit price	Number	Total price	Unit price	Number	Total price
	4851.12	1	4851.12	4851.12	1	4851.12
Safety monitoring systems	Unit price	Number	Total price	Unit price	Number	Total price
	0.00	0	0.00	12,127.80	1	12,127.80
Control systems	Unit price	Number	Total price	Unit price	Number	Total price
	0.00	0	0.00	1774.80	1	1774.80
Total amount	25,557.12			39,459.72		

Table 7
Maintenance costs of systems (Unit is in USD).

Item	Existing conventional ventilation			TVIC		
Fans	Unit price	Number	Total price	Unit price	Number	Total price
	0	2	0	0	2	0
VFD	Unit price	Number	Total price	Unit price	Number	Total price
	0	0	0	0	2	0
Safety monitoring systems	Unit price	Number	Total price	Unit price	Number	Total price
	0	0	0	1405.05	1	1405.05
Control systems	Unit price	Number	Total price	Unit price	Number	Total price
	0	0	0	118.32	1	118.32
Total amount	0			1523.37		

the addition of these devices. Table 6 shows the detailed installation cost and material cost for the Huayingshan Tunnel. In addition, these devices also incur maintenance costs during the operational period. Maintenance costs are primarily related to the parts replacement costs. Table 7 shows the detailed parts replacement costs. By combining the electricity charge in the field (calculated by the energy consumption in Fig. 11) and the additional initial investment discussed above, the cost increase trend of the ventilation system can be mapped (see Fig. 12). The solid line in the figure is the actual electricity consumption, and the

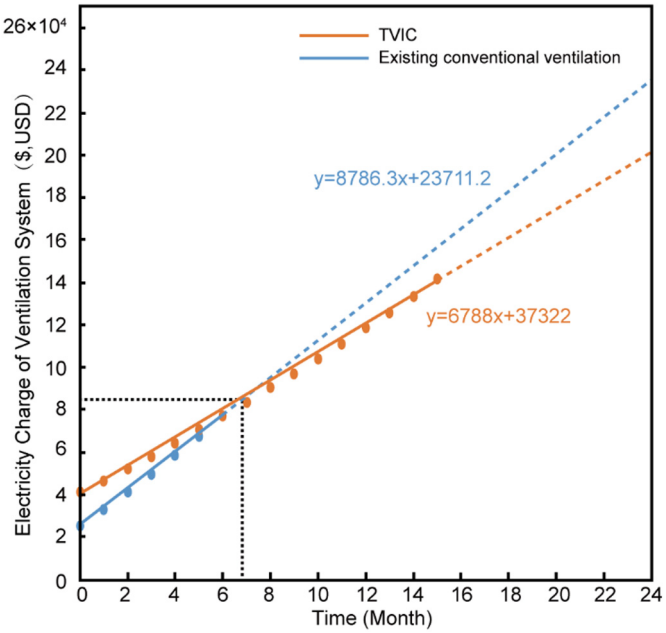

Fig. 12. Cost trends for TVIC and conventional ventilation method.

Table 8
Comparison with typical fan control system using sensors.

	TVIC	Reference [57]	Reference [5]	Reference [58]
Purpose	Ventilation system control during tunnel construction	Ventilation system control during tunnel construction	Ventilation system control during tunnel operation period	Ventilation system control for public and industrial buildings
Control method	RBF NN	Fuzzy control	Feed-forward control structure with an adaptive logic	LLVM-based ANN
System costs	$15,425.97	$64,126.00	Not given	Not given
Power saving rate	42%	18%	50%	Not given
Application	Field application in Huayingshan Tunnel	Field application in Guanhuchong Tunnel	Field application in Blanka Tunnel	Laboratory stage

dotted line is an extension of a solid line, representing the predicted electricity consumption. It can be seen that the investment in the ventilation system using TVIC is higher than that without TVIC, but the total charges are almost the same at around the seventh month. Over a longer usage period, the benefits of TVIC thus become more obvious. At present, most tunnels still adopt the manual control mode to adjust the fan operating frequency in order to achieve energy savings in the field. Only a few studies [57] have reported that the fan operating frequency can be adjusted by monitoring the change of gas concentration. A comparison between different control methods for the fan control system is shown in Table 8. It can be observed that TVIC offers clear energy-saving advantages.

Technically, there is no need to ventilate during construction for a tunnel < 150 m. At present, tunneling speeds have reached 100 m/month. Considering the tunneling speed and initial investment, TVIC is not a wise choice in this situation which involves a unidirectional tunneling tunnel with a length of about 850 m or a bidirectional tunneling tunnel with a length of about 1700 m. Therefore, TVIC is preferred for use in long tunnels. The longer the tunnel, the greater the energy savings that are realized. Besides, for other long tunnels, environmental parameters may be different from those of the Huayingshan Tunnel, so the TDS needs to be re-acquired according to the TDS acquisition rules to train the neural network that is suitable for its own case. The training method, the composition of the hardware, and the software remains the same as the Huayingshan tunnel. In the next step, the self-learning ability of TVIC should be enhanced to ensure that it is optimized for the relevant application.

5. Conclusions

In this study, TVIC was developed and applied in the Huayingshan Tunnel. It modifies the operating frequency of the fan according to the pollutant concentrations, temperature, and tunnel length, as well as improves the reliability and sensitivity of the ventilation system. This study can be summarized as follows:

A set of TDS acquisition rules is established based on existing regulations requirements, and these rules are used to train the RBF NN. The mapping between the tunnel environment and fan operating frequency is determined. A hardware/software co-design is required for the implementation of the function.

Field application results indicate that TVIC achieves energy savings with respect to fan operations. Compared with the manual control mode, TVIC reduces electricity consumption by nearly 42%. Moreover, the system displays excellent stability during the overall construction. In addition, the hardware composition of TVIC is commercially available. In combination with the RBF NN training discussed above, the method proposed in this paper can be seamlessly reused in other tunnels. In future studies, the self-learning ability of TVIC should be enhanced for optimization in the relevant applications.

Acknowledgements

This work was financially supported by the Fundamental Research Funds for the Central Universities (2018CDXYTM0003), Special Funding for Postdoctoral Research Projects in Chongqing (XmT2018011), and Natural Science Foundation of Chongqing (cstc2019jcyj-xfkxX0001).

References

[1] Z.Q. Zhang, H. Zhang, Y.J. Tan, H.Y. Yang, Natural wind utilization in the vertical shaft of a super-long highway tunnel and its energy saving effect, Build. Environ. 145 (2018) 140–152, https://doi.org/10.1016/j.buildenv.2018.08.062.
[2] S. Bogdan, B. Birgmajer, Z. Kovacic, Model predictive and fuzzy control of a road tunnel ventilation system, Transportation Research Part C: Emerging Technologies 16 (5) (2008) 574–592, https://doi.org/10.1016/j.trc.2007.11.004.
[3] P.H. Chen, J.H. Lai, C.T. Lin, Application of fuzzy control to a road tunnel ventilation system, Fuzzy Sets Syst. 100 (1–3) (1998) 9–28, https://doi.org/10.1016/S0165-0114(97)00209-1.
[4] E. Karakas, The control of highway tunnel ventilation using fuzzy logic, Eng. Appl. Artif. Intell. 16 (7–8) (2003) 717–721, https://doi.org/10.1016/S0952-1976(03)00068-X.
[5] J. Šulc, L. Ferkl, J. Cigler, J. Pořízek, Optimization-based control of ventilation in a road tunnel complex, Control. Eng. Pract. 69 (2017) 141–155, https://doi.org/10.1016/j.conengprac.2017.09.011.
[6] S. Shao, X.G. Yang, J.W. Zhou, Numerical analysis of different ventilation schemes during the construction process of inclined tunnel groups at the Changheba Hydropower Station, China, Tunn. Undergr. Space Technol. 59 (2016) 157–169, https://doi.org/10.1016/j.tust.2016.07.007.
[7] R. Rodríguez, C. Lombardía, Analysis of methane emissions in a tunnel excavated through carboniferous strata based on underground coal mining experience, Tunn. Undergr. Space Technol. 25 (4) (2010) 456–468, https://doi.org/10.1016/j.tust.2010.02.010.
[8] M.J. Liu, Q.G. Deng, F.J. Zhao, Y.W. Liu, Origin of hydrogen sulfide in coal seams in China, Saf. Sci. 50 (4) (2012) 668–673, https://doi.org/10.1016/j.ssci.2011.08.054.
[9] R. Rodríguez, M.B. Díaz-Aguado, C. Lombardía, Compensation of CH_4 emissions during tunneling works in Asturias: a proposal with benefits both for local councils and for the affected population, J. Environ. Manag. 104 (15) (2012) 175–185, https://doi.org/10.1016/j.jenvman.2012.03.020.
[10] M.C. Jena, S.K. Mishra, H.S. Moharana, Experimental investigation on power consumption of an industrial fan with different flow control methods, Environ. Prog. Sustain. Energy 39 (1) (2020) 1–9, https://doi.org/10.1002/ep.13237.
[11] D.M. Hargreaves, I.S. Lowndes, The computational modeling of the ventilation flows within a rapid development drivage, Tunn. Undergr. Space Technol. 22 (2) (2007) 150–160, https://doi.org/10.1016/j.tust.2006.06.002.
[12] A. Chatterjee, L.J. Zhang, X.H. Xia, Optimization of mine ventilation fan speeds according to ventilation on demand and time of use tariff, Appl. Energy 146 (15) (2015) 65–73, https://doi.org/10.1016/j.apenergy.2015.01.134.
[13] I.S. Lowndes, Z.Y. Yang, S. Jobling, C. Yates, A parametric analysis of a tunnel climatic prediction and planning model, Tunn. Undergr. Space Technol. 21 (5) (2006) 520–532, https://doi.org/10.1016/j.tust.2005.08.012.
[14] C. Guo, M.N. Wang, L. Yang, Z.T. Sun, Y.L. Zhang, J.F. Xu, A review of energy consumption and saving in extra-long tunnel operation ventilation in China, Renew. Sust. Energ. Rev. 53 (2016) 1558–1569, https://doi.org/10.1016/j.rser.2015.09.094.
[15] E. Ozdemir, Energy conservation opportunities with a variable speed controller in a boiler house, Appl. Therm. Eng. 24 (7) (2004) 981–993, https://doi.org/10.1016/j.applthermaleng.2003.11.009.
[16] M. Teitel, A. Levi, Y. Zhao, M. Barak, E. Bar-lev, D. Shmuel, Energy saving in agricultural buildings through fan motor control by variable frequency drives, Energ Buildings 40 (6) (2008) 953–960, https://doi.org/10.1016/j.enbuild.2007.07.010.
[17] G.E. Du Plessis, L. Liebenberg, E.H. Mathews, The use of variable speed drives for cost-effective energy savings in South African mine cooling systems, Appl. Energy 111 (2013) 16–27, https://doi.org/10.1016/j.apenergy.2013.04.061.
[18] A.T. de Almeida, P. Fonseca a, P. Bertoldi, Energy-efficient motor systems in the industrial and in the services sectors in the European Union: characterisation, potentials, barriers and policies, Energy 28 (7) (2003) 673–690, https://doi.org/10.1016/S0360-5442(02)00160-3.

[19] M.B. Massanés, L.S. Pera, J.O. Moncunill, Ventilation management system for underground environments, Tunn. Undergr. Space Technol. 50 (2015) 516–522, https://doi.org/10.1016/j.tust.2015.09.001.
[20] M. Teitel, Y. Zhao, M. Barak, E. Bar-lev, D. Shmuel, Effect on energy use and greenhouse microclimate through fan motor control by variable frequency drives, Energy Convers. Manag. 45 (2) (2004) 209–223, https://doi.org/10.1016/S0196-8904(03)00147-X.
[21] E. Al-Bassam, R. Alasseri, Measurable energy savings of installing variable frequency drives for cooling towers' fans, compared to dual speed motors, Energ Buildings 67 (2013) 261–266, https://doi.org/10.1016/j.enbuild.2013.07.081.
[22] I.M. Alsofyani, N.R.N. Idris, A review on sensorless techniques for sustainable reliablity and efficient variable frequency drives of induction motors, Renew. Sust. Energ. Rev. 24 (2013) 111–121, https://doi.org/10.1016/j.rser.2013.03.051.
[23] P. Miller, B. Olateju, A. Kumar, A techno-economic analysis of cost savings for retrofitting industrial aerial coolers with variable frequency drives, Energy Convers. Manag. 54 (1) (2012) 81–89, https://doi.org/10.1016/j.enconman.2011.09.018.
[24] G. Shim, L. Song, G. Wang, Comparison of different fan control strategies on a variable air volume system through simulations and experiments, Build. Environ. 72 (2014) 212–222, https://doi.org/10.1016/j.buildenv.2013.11.003.
[25] C.C. Chang, S.S. Shieh, S.S. Jang, C.W. Wu, Y. Tsou, Energy conservation improvement and ON–OFF switch times reduction for an existing VFD-fan-based cooling tower, Appl. Energy 154 (2015) 491–499, https://doi.org/10.1016/j.apenergy.2015.05.025.
[26] China Merchants Chongqing Communications Technology Research, TG/T D70/2-02-2014: Guidelines for Design of Ventilation of Highway Tunnel, Ministry of Transport of the People's Republic of China, China Communications Press Co., Ltd, Beijing, China, 2014, pp. 23–28 http://xxgk.mot.gov.cn/jigou/glj/201407/t20140730_2978975.html.
[27] K. Wu, Q.M. Yang, C. Kang, X. Zhang, Z.Y. Huang, Adaptive critic design based control of tunnel ventilation system with variable jet speed, Journal of Signal Processing Systems 86 (2017) 269–278, https://doi.org/10.1007/s11265-016-1123-8.
[28] M. Król, A. Król, P. Koper, P. Wrona, Full scale measurements of the operation of fire ventilation in a road tunnel, Tunn. Undergr. Space Technol. 70 (2017) 204–213, https://doi.org/10.1016/j.tust.2017.07.016.
[29] F.R. Mazarrón, C. Porras-Amores, I. Cañas-Guerrero, Annual evolution of the natural ventilation in an underground construction: influence of the access tunnel and the ventilation chimney, Tunn. Undergr. Space Technol. 49 (2015) 188–198, https://doi.org/10.1016/j.tust.2015.04.015.
[30] A. Pflitsch, M. Bruene, B. Steiling, M. Killing-Heinze, B. Agnew, Air flow measurements in the underground section of a UK light rail system, Appl. Therm. Eng. 32 (2012) 22–30, https://doi.org/10.1016/j.applthermaleng.2011.07.030.
[31] C.Q. Liu, W. Nie, Q. Bao, Q. Liu, C.H. Wei, Y. Hua, The effects of the pressure outlet's position on the diffusion and pollution of dust in tunnel using a shield tunneling machine, Energ Buildings 176 (2018) 232–245, https://doi.org/10.1016/j.enbuild.2018.06.046.
[32] X.B. Kang, M. Xu, S. Luo, Q. Xia, Study on formation mechanism of gas tunnel in non-coal strata, Nat. Hazards 66 (2) (2013) 291–301, https://doi.org/10.1007/s11069-012-0484-y.
[33] R. Li, Y. Meng, H.B. Fu, L.W. Zhang, X.N. Ye, J.M. Chen, Characteristics of the pollutant emissions in a tunnel of Shanghai on a weekday, J. Environ. Sci. 71 (2018) 136–149, https://doi.org/10.1016/j.jes.2017.11.015.
[34] J.L. Lang, Y. Zhou, S.Y. Cheng, Y.Y. Zhang, M. Dong, S.Y. Li, G. Wang, Y.L. Zhang, Unregulated pollutant emissions from on-road vehicles in China, 1999-2014, Sci. Total Environ. 573 (2016) 974–984, https://doi.org/10.1016/j.scitotenv.2016.08.171.
[35] X.Y. He, Y. Jiang, Review of hybrid electric systems for construction machinery, Autom. Constr. 92 (2018) 286–296, https://doi.org/10.1016/j.autcon.2018.04.005.
[36] T.L. Lin, L. Wang, W.P. Huang, H.L. Ren, S.J. Fu, Q.H. Chen, Performance analysis of an automatic idle speed control system with a hydraulic accumulator for pure electric construction machinery, Autom. Constr. 84 (2017) 184–194, https://doi.org/10.1016/j.autcon.2017.09.001.
[37] S.Y Zhou, Master Thesis, Research on Main Drive Motor Control System of Pure Electric-Driven Construction Machinery, College of Mechanical Engineering and Automation, Huaqiao University, 2019, https://kns.cnki.net/KCMS/detail/detail.aspx?dbcode=CMFD&dbname=CMFD202001&filename=1019626012.nh&uid=WEEvREcwSlJHSldRa1FhcTdnTnhYaCs3RmZWUGgvMzFNVnJ6STJyeU1DWT0.
[38] S.Y. Cai, Z.L. Ma, M.J. Skibniewski, S. Bao, Construction automation and robotics for high-rise buildings over the past decades: a comprehensive review, Adv. Eng. Inform. 42 (2019) 1–18, https://doi.org/10.1016/j.aei.2019.100989 100989.
[39] Z. Liu, X.L. Wang, Z.F. Cheng, R.R. Sun, A.L. Zharig, Simulation of construction ventilation in deep diversion tunnels using Euler-Lagrange method, Comput. Fluids 105 (2014) 28–38, https://doi.org/10.1016/j.compfluid.2014.09.016.
[40] J. Toraño, S. Torno, M. Menendez, M. Gent, J. Velasco, Models of methane behaviour in auxiliary ventilation of underground coal mining, Int. J. Coal Geol. 80 (1) (2009) 35–43, https://doi.org/10.1016/j.coal.2009.07.008.
[41] Y. Fang, J.G. Fan, B. Kenneally, M. Mooney, Air flow behavior and gas dispersion in the recirculation ventilation system of a twin-tunnel construction, Tunn. Undergr. Space Technol. 58 (2016) 30–39, https://doi.org/10.1016/j.tust.2016.04.006.
[42] C. Cao, J.Y. Zhao, H.G. Ding, Dust removal of large cross-section tunnels: following ventilation and its adjustment strategy, J. Braz. Soc. Mech. Sci. Eng. 40 (10) (2018) 1–14, https://doi.org/10.1007/s40430-018-1403-2.
[43] Q. Li, C. Chen, H.T. Yuan, L.Y. Wang, S.H. Xu, Y.R. Li, Prediction of pollutant concentration and ventilation control in urban bifurcate tunnel, China, Tunn. Undergr. Space Technol. 82 (2018) 406–415, https://doi.org/10.1016/j.tust.2018.06.002.
[44] A.H. Zhang, L. Zhang, RBF neural networks for the prediction of building interference effects, Comput. Struct. 82 (27) (2004) 2333–2339, https://doi.org/10.1016/j.compstruc.2004.05.014.
[45] Z. Majdisova, V. Skala, Radial basis function approximations: comparison and applications, Appl. Math. Model. 51 (2017) 728–743, https://doi.org/10.1016/j.apm.2017.07.033.
[46] R.A. Tenenbaum, F.O. Taminato, V.S.G. Melo, Fast auralization using radial basis functions type of artificial neural network techniques, Appl. Acoust. 157 (2020) 1–8, https://doi.org/10.1016/j.apacoust.2019.07.041 106993.
[47] F. Shi, H. Wang, L. Yu, F. Hu, MATLAB Intelligent Algorithm 30 Cases Analysis, 1st, Beihang University Press, 2011, pp. 237–247.
[48] D.Q. Zhang, G.M. Zang, J. Li, K.P. Ma, H. Liu, Prediction of soybean price in China using QR-RBF neural network model, Comput. Electron. Agric. 154 (2018) 10–17, https://doi.org/10.1016/j.compag.2018.08.016.
[49] I. Czarnowski, P. Jedrzejowicz, Designing RBF networks using the agent-based population learning algorithm, N. Gener. Comput. 32 (3–4) (2014) 331–351, https://doi.org/10.1007/s00354-014-0408-3.
[50] Q.F. He, H. Shahabi, A. Shirzadi, S.J. Li, W. Chen, N.Q. Wang, H.C. Chai, H.Y. Bian, J.Q. Ma, Y.T. Chen, X.J. Wang, K. Chapi, B. Bin Ahmad, Landslide spatial modelling using novel bivariate statistical based Naïve Bayes, RBF classifier, and RBF network machine learning algorithms, Sci. Total Environ. 663 (2019) 1–15, https://doi.org/10.1016/j.scitotenv.2019.01.329.
[51] Ltd China Railway Eryuan Engineering Group Co., TB 10120-2019: Technical Code for Railway Tunnel with Gas, National Railways Administration of the P.R.C, Beijing, China, 2019, pp. 16–18 http://www.nra.gov.cn/xwzx/xwdt/xwlb/201905/t20190520_78684.shtml.
[52] State Administration of Work Safety, State Administration of Coal Mine Safety, Safety Regulations in Coal Mine, China Coal Industry Publishing House, Beijing, 2016, pp. 29–101 http://www.chinasafety.gov.cn/fw/flfgbz/gz/201603/t20160325_233479.shtml.
[53] A. Barati-Harooni, A. Najafi-Marghmaleki, An accurate RBF-NN model for estimation of viscosity of nanofluids, J. Mol. Liq. 224 (2016) 580–588, https://doi.org/10.1016/j.molliq.2016.10.049.
[54] A. Sharma, Guided stochastic gradient descent algorithm for inconsistent datasets, Appl Soft Comput 73 (2018) 1068–1080, https://doi.org/10.1016/j.asoc.2018.09.038.
[55] N.P. Thanh, Y.S. Kung, S.C. Chen, H.H. Chou, Digital hardware implementation of a radial basis function neural network, Comput. Electr. Eng. 53 (2016) 106–121, https://doi.org/10.1016/j.compeleceng.2015.11.017.
[56] Y.S. Kung, H. Than, T.Y. Chuang, FPGA-realization of a self-tuning PID controller for X-Y table with RBF neural network identification, Microsyst. Technol. 24 (2018) 243–253, https://doi.org/10.1007/s00542-016-3248-x.
[57] X.G. Lin, Research on numerical simulation and automatic control technology of tunnelling ventilation, Master Thesis College of Resources and Safety Engineering, Central South University, https://kns.cnki.net/KCMS/detail/detail.aspx?dbcode=CMFD&dbname=CMFD201501&filename=1014406784.nh&uid=WEEvREcwSlJHSldRa1FhcTdnTnhYaCs3RmZWUGgvMzFNVnJ6STJyeU1DWT0, (2014).
[58] C. Ren, S.J. Cao, Implementation and visualization of artificial intelligent ventilation control system using fast prediction models and limited monitoring data, Sustain. Cities Soc. 52 (2020) 1–14, https://doi.org/10.1016/j.scs.2019.101860.